





# Optimal Control and Grasping for a Robotic Hand with a Non-linked Double Tendon Arrangement

Erick J. Sánchez-Garnica , Liliam Rodríguez-Guerrero , Rocío Ortega-Palacios ,  
and Omar Jacobo Santos-Sánchez 

**Abstract**—After comparing different robotic hand projects, a problem is identified: when a finger has a degree of freedom, the hand is unable to grasp irregularly shaped objects. This article proposes a solution. The use of a non-linked double-tendon arrangement in the fingers allows them to have free movement; coupled with the use of Inertial Measurement Units to determine its position, ensures that, despite having one degree of freedom per finger, the hand can effectively grasp irregular objects. Additionally, a web application is developed to control hand movements through voice commands. Finally, due to the necessity for these types of devices to be mobile, an optimal control law is used to minimize energy consumption, thereby increasing autonomy when the hand is powered by batteries. As an additional note, the conducted experiments reveal that the movement of all fingers occurs simultaneously, demonstrating that parallel multitasking programming techniques effectively fulfill that purpose.

**Link to graphical and video abstracts, and to code:**  
<https://latam.ieceer9.org/index.php/transactions/article/view/8484>

**Index Terms**—Control theory, Robotic hand, Optimal PI, Web application

## I. INTRODUCTION

The human hand performs mainly two functions: touch (push) and grip; so a robotic hand must also perform them. It is important to mention that the thumb represents the most important element of the hand. Without this finger the functional capacity of the hand is reduced by about 40%, which is why its movements should be an essential aspect in the development of functional robotic hand [1].

The construction of artificial hands has been present in our history for several millennia. The advent of industrial technology has also affected this sector, which is why there have been records of robotic hands for more than a century [2]. The areas in which these devices have been implemented are very diverse, just to mention a few are industrial automation, medical robotics, assistive technology, research and development and space exploration.

Around the world there are various companies that are dedicated to the design and construction of robotic

hands, among which are; Robotis [3], a leading Korean company in educational robotics and the development of robotic technology, including advanced robotic hands; UK company Shadow Robot [4], whose products have up to 20 degrees of freedom (DOF) and can be manipulated remotely; Barrett Technology from USA [5], whose model BH8-282 BarrettHand is a highly sensitive gripper device; Robotiq [6], a German company that offers various automation devices, including different DOF grippers; Yujin Robot [7], a Korean company specializing in robotics, has developed advanced robotic hands as part of its diverse range of robotic solutions; among others. It is important to mention that all these companies are of an industrial nature, so their prices are high, which represents a barrier for academic communities to have access to them, so it is important to find more affordable solutions to these realities. Fortunately, so-called open source initiatives have been created, making it possible to incorporate and adapt the technology in an accelerated and low-cost manner.

Going deeper into open source projects, in [8]–[11], it is possible to observe various designs of robotic hands actuated by motors, however, manually manipulated without using sensors to determine the position of the fingers and without closed-loop control. In [12] a robotic hand with servomotors to move the fingers is presented, however it does not consider any sensor to identify their position. For more open-source community projects [13] can be consulted.

Also, research projects like [14]–[16] have been developed. In those works, an open source CAD design of a hand was printed and a hybrid control (voice-myoelectric) was used to achieve the individual opening and closing of the thumb and the remaining four fingers, however, the applied ON-OFF type control limits the functionality of the robotic hand. In [17] a hand controlled by various types of signals is presented, these are encephalographic, myoelectric, voice and gestures, the project provides a comprehensive explanation of the methods used to acquire the different signals; however, to move the hand, a control law is not used, that is, it is an open loop system. In [18], [19], it was also observed that they use myoelectric sensors as triggers of the control action. In [20]–[23], a hand prototype with five fingers divided into three parts (phalanges), joined by a small pulleys system is presented, in which, to perform the bending movement a direct current motor is used at the base, which acts on a wire (or cable) which runs through the inside of the finger and

Erick J. Sánchez-Garnica, Liliam Rodríguez-Guerrero and Omar Jacobo Santos-Sánchez are with Universidad Autónoma del Estado del Hidalgo, Mineral de la Reforma, Hidalgo, México (e-mail: sa106434@uaeh.edu.mx, liliam\_rodriguez@uaeh.edu.mx and omarj@uaeh.edu.mx).

Rocío Ortega-Palacios is with Universidad Politécnica de Pachuca, Zempoala, Hidalgo, México (e-mail: rortega@upp.edu.mx).

connects to the distal phalanx. For the extension movement, a set of springs is used. Unlike the previous ones, in [24] a double cable arrangement (tendons) is used to perform both extension and flexion movements. Additionally, in [25] it is possible to see an exhaustive comparison between various finger models, among which some are tendon-driven.

Table I shows a comparison between different linkage-driven finger mechanism projects. It can be seen that the article presents the mechanical design, the control law used, the number of degrees of freedom (DOF) that a finger presents (measured from the number of actuators involved), the hand's ability to hold irregular objects, and the sensor and actuator used. It is important to mention that all the projects have a physical prototype, with the exception of [22], [23].

From Table I, it can be seen that when the fingers have one DOF, the hand is not able to hold irregular objects (shape adaptive). When it comes to control strategies, it has been found that projects like [18], [22] use inverse kinematics to determine the position of the fingers. However, this process assumes that the angles between the phalanges are known. This is achieved by conditioning the trajectory of flexion and extension movements to always be the same.

In this article, a robotic hand is developed based on the Inmoov hand, a 3D model given in [24], which includes five fingers with one DOF and 3 phalanges each. Using two tendons per finger (one for extension and another for flexion) with no end-to-end connection (which means that the ends at the distal phalanx are not joined), generates a free trajectory, which offers the possibility to grab irregular objects. In [33], it is explained that in order to grab an irregular object, it is necessary that the fingers present free movement. To determine finger position, an Inertial Measurement Unit (IMU) is incorporated over the distal phalanx, and an Optimal PI Controller [34] is used to move them at the desire setpoint position. Furthermore, a force-sensitive resistor (FSR) sensor [35] is included in the palm of the hand in order to measure the pressure exerted by it and to improve the grip, all this, managed with an ESP32 Microcontroller Unit (MCU). Additionally, the use of voice commands, indicating them through a web application, is proposed.

Moreover, the current rise of the Internet of Things (IoT) has generated that smartphones are used by most people, which is why the use of voice commands could be a viable option to be considered.

The contributions of the article are the following:

- 1) Free movement in fingers of one DOF is achieved by the non-linked double tendon arrangement and the incorporation of IMUs to measure their position.
- 2) Use an optimal PI control strategy for the closed-loop system, which minimizes a quadratic performance criteria that depends on finger position, providing potential energy savings, having a positive impact on mobility,

since it allows elements, such as batteries to last longer when compared with other tuning methods.

- 3) The implementation of an IoT-based approach, such as voice commands to control hand movements, constitutes a distinct advantage when compared to other projects with similar features.
- 4) Technical validation of the open source project Inmoov with the optimal PI control applied to the fingers of the artificial hand.

This article is organized as follows. Section II presents the mechanical and electronic components that make up the device, as well as the programming technique used. The system identification and the mathematical model are shown in the Section III. The control strategy is provided in Section IV. The implementation details of the control laws and experimental results are addressed in Section V. Finally, some concluding comments are given in Section VI.

## II. CONSTRUCTION OF THE ROBOTIC HAND

This section shows the 3D model used in this project as well as the electronic and power interfaces needed for the servomotor function.

The right hand 3D printable model was obtained from Inmoov project [24], which consists of five tendon-driven fingers, each one actuated by a servomotor and capable of holding irregular objects due to the free movement achieved by the non-linked double tendon arrangement. Despite the fact that the fingers are divided into three phalanges, due to hardware limitations, it is not possible to place a motor in each of them, which leads to these having one DOF [36], and therefore, the whole hand is a five DOF system.

Polylactic Acid (PLA) was used to print the hand. This material offers both resistance and easy to print by a 3D, non-industrial, printer. The printing time of all pieces was about 76 hours, using a 0.4 mm nozzle and an Ender 3 Pro printer.

Each tendon-driven finger is actuated by a servomotor (MG995 [37]), which is controlled by a Pulse-Width Modulation (PWM) signal. This signal is the control input to the actuator whose details are presented in the Section IV.

To measure the finger position on space, a MPU6050 sensor [38] is used. This sensor has a built-in accelerometer and gyroscope; both were used to get the upper phalanx inclination of each finger.

To calculate a valid approximation of the finger position, it is necessary to obtain the sensor inclination in the range  $[0^\circ, 360^\circ]$ . This is because, for the complete movement of the finger, the sensor goes from a face-up to a face-down position or vice versa. Since this range is not the default for

TABLE I  
COMPARISON OF LINKAGE-DRIVEN FINGER MECHANISM PROJECTS

Article	Control strategy	DOF	Shape adaptive	Sensor	Actuator
[26]	Manually operated	One	No	No	Servomotor
[20]	Fuzzy Proportional Integral Derivative controller	One	No	Force Sensitive Resistor (FSR)	DC motor
[27]	Manually operated	Three	Yes	No	DC motor
[21]	Digital Signal Processing (DSP) based controller	Two	Yes	Potentiometer	DC motor
[28]	Manually operated	Two	Yes	Pressure	Hidraulic pump
[22]	Sliding mode and impedance controller	One	No	No	DC motor
[29]	Manually operated	One	No	No	DC motor
[23]	DSP-based controller that estimates finger position	One	No	No	DC motor
[30]	Manually operated	Three	Yes	No	Linear actuator
[18]	Proportional Integral Derivative (PID) controller	One	No	Myoelectric	DC motor
[31]	Manually operated	Two	Yes	FSR	DC motor
[19]	On-Off controller	Two	No	Myoelectric	DC motor
[32]	Manually operated	Two	Yes	No	Servomotor

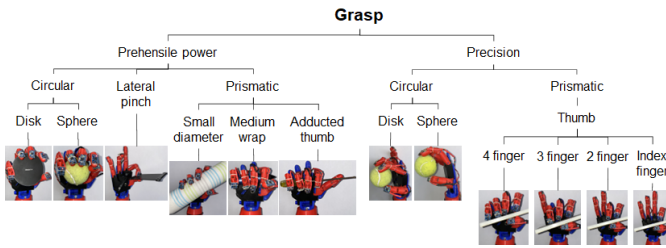


Fig. 1. Cutkosky grasp types that the prototype can perform.

it, it was necessary to compute a transformation based on the accelerometer reading. The following relations are proposed:

$$\begin{aligned} x &= 180/\pi [\arctan(-y_{ang}/-z_{ang}) + \pi], \\ y &= 180/\pi [\arctan(-x_{ang}/-z_{ang}) + \pi], \\ z &= 180/\pi [\arctan(-y_{ang}/-x_{ang}) + \pi], \end{aligned} \quad (1)$$

where  $x_{ang}$ ,  $y_{ang}$ ,  $z_{ang}$  are the accelerometer angles in range  $[-90^\circ, 90^\circ]$  and  $x$ ,  $y$ ,  $z$  are the compute position angles in range  $[0^\circ, 360^\circ]$ . It is important to mention that these equations present a singularity around  $360^\circ$ ; however, this does not present a problem since the actual operating range of the finger is  $[0^\circ, 250^\circ]$

To know the range of movements and actions that a robotic hand can perform, the Cutkosky taxonomy [39], which is a collection of 16 grasp types, was used to verify the prototype. The hand can execute 12 of the 16 Cutkosky grasps, which represents a compliance factor of 75%. Fig. 1 shows the Cutkosky grasp types that the prototype can perform.

In order to the user could manipulate the hand (client), a web dashboard has been developed (server). Both systems communicate with each other through a Message Queue

Telemetry Transport (MQTT) server [40], while the client communicates with the prototype via Inter Integrated Circuits (I<sup>2</sup>C) protocol [41]. The IMUs and the servomotors also used this to communicate with the MCU. Google's Speech-to-text<sup>®</sup> service [42] was used, allowing the user to use predetermined voice commands, each of which is translated into a set of five angles (positions) and sent to the MCU as a setpoint for each finger. Table II shows an example of the positions established for the main coded voice commands that were loaded on the server. Under this standard, it is possible to load more commands to be interpreted by the system.

TABLE II  
MAIN VOICE COMMANDS AND THEIR RESPECTIVE ANGLES

Command	Index	Middle	Ring	Little	Thumb
<b>Open hand</b>	0°	0°	0°	0°	0°
<b>Close hand</b>	250°	250°	220°	220°	200°
<b>Claw</b>	160°	160°	150°	150°	140°
<b>Number one</b>	0°	250°	220°	220°	200°
<b>Number two</b>	0°	0°	220°	220°	200°

Putting it all together, Fig. 2 shows a graphical representation of this architecture, whose operation is described as follows: The user dictates a voice command that is interpreted by the speech-to-text service, the web app translates the command to the corresponding setpoints and sends it to the MCU through the MQTT server, the controller sends the necessary signals to the fingers so that they begin their movement toward the indicated setpoints.

In the initial experiments, the MCU was able to control one finger; however, the movement trajectory of five fingers, tested at same time, exhibits irregular and discontinuous changes, due to insufficient data processing speed, which is overcome

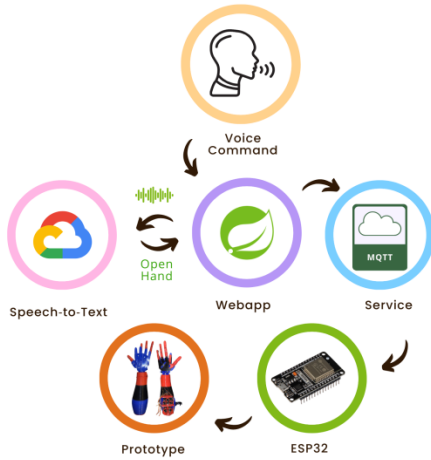


Fig. 2. Project's global communication architecture.

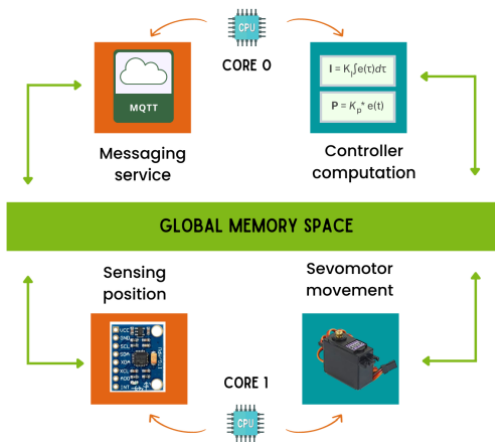


Fig. 3. Multitasking and parallel programming schema.

by implementing multitasking and parallel programming. This was possible since the ESP32 is a dual-core MCU. Four tasks are defined, each of them are assigned to a specific core:

- 1) Sensor reading and computation of finger position (core 1): Using the I<sup>2</sup>C protocol, the IMU obtains the acceleration and angular velocity of the accelerometer and gyroscope, respectively; with which it calculates the position of the finger through the relations (1).
- 2) Controller output computes (core 0): Through an optimal PI control, the duty cycle that must be applied to the servomotor is calculated.
- 3) Servomotor movement (core 1): The calculated duty cycle value is applied to the servomotor, which moves accordingly.
- 4) MQTT messaging system (core 0): A passive connection is maintained with the MQTT server, which allows for the reception and production of messages, which will serve to communicate with the web application.

Fig. 3 shows the tasks distribution over the MCU cores. It can be seen that in each core, a task with low and another with high computational demand was assigned, which allows maintaining a balance in the load of each core.

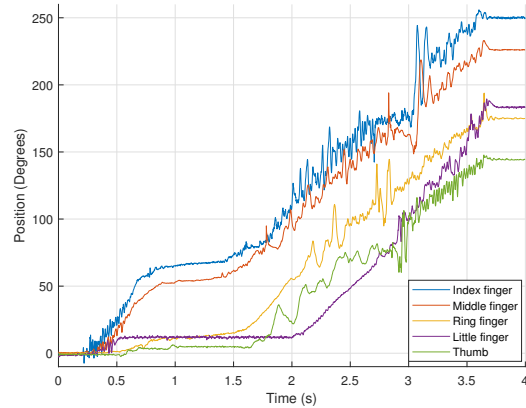


Fig. 4. Fingers' unit step response chart.

### III. MATHEMATICAL MODEL AND FINGER'S IDENTIFICATION

As could be seen in the data presented in Table I, the use of a kinematic model in conjunction with one DOF finger does not allow free movement, making it impossible to grasp irregular objects. In order to address this issue, it was imperative to model the finger utilizing a technique that did not rely on knowledge of the angles between the phalanges. Therefore, identification through unit step response, specifically a transfer function, was chosen.

The whole hand is a nonlinear dynamic system, however, every finger can be modeled as a linear system working in an operation region, whose first order transfer function with time delay is given by

$$G(s) = \frac{X(s)}{U(s)} = \frac{b}{s+a} e^{-Ls}, \quad (2)$$

where  $U(s)$  is the input (representing the duty cycle of the PWM sent to the servomotor controller),  $X(s)$  is the output system (represents the position of the distal phalanx measured in degrees from the IMU),  $L > 0$  is the delay and it is measured in ms,  $a$  and  $b$  are the finger constant parameters. Fig. 4 shows the unit step response for each finger.

The delay arises in the system because the tendons cannot be fully tensioned due to the mechanical characteristics of the hand. It is important to note that this delay is not large enough; however, it has been retained to align with the algorithm employed in this article.

Considering transfer function (2) and the results shown in Fig. 4, parameters for each finger are calculated, and their values are presented in Table III. It is crucial to emphasize that the mathematical model described in Equation (2) remains valid throughout the operational range of the fingers, demonstrating consistent and suitable behavior (experimental validation supporting this claim is provided in Section V).

TABLE III  
TRANSFER FUNCTION PARAMETERS FOR EACH FINGER

Finger	a	b	L
Index	0.4264	0.0888	0.209
Middle	0.3587	0.0730	0.264
Ring	0.3949	0.0576	0.148
Little	0.3546	0.0541	0.287
Thumb	0.3772	0.0453	0.207

#### IV. APPLIED CONTROL STRATEGY: OPTIMAL PI CONTROL

Although there are various control techniques, when it comes to first-order plants, state feedback control is usually the best option, since it is capable of stabilizing a system, at a desire setpoint, by adjusting the input in terms of the output signal. This, added to the fact that it is desirable for a robotic hand to be battery operated, makes it necessary for its power consumption to be minimal in order to maximize its autonomy. For this reason, it has been decided to use an optimal PI controller.

The approach of this type of controller has been extensively studied for linear systems in both continuous and discrete time. A more in-depth analysis on this can be found in [43] and [44].

The control strategy used in this paper is given in [34], where it is mentioned that a PI control is the correct feedback regulator for first-order plants with an input delay. An application of this type of control is presented in [45]. It is important to emphasize that the derivative part of the controller is not employed, as oscillations in the closed-loop finger response are not desired. Consider a unity output feedback of the form



where  $C(s) = \frac{U(s)}{E(s)} = K_p + \frac{K_i}{s}$  is the controller; for feedback design, the external setpoint does not affect the result, so it is set to zero ( $r = 0$ ); since  $e(t) = -x(t)$ , from (2) and applying the inverse Laplace transform the dynamic error equation is given by

$$\dot{e}(t) = -ae(t) - bu(t - L) \quad (3)$$

Defining the state variables as  $x_1(t) = \int_0^t e(\tau) d\tau$  and  $x_2(t) = e(t)$ , such that  $x(t) = [x_1(t), x_2(t)]^T$ , then

$$\begin{aligned} \dot{x}_1(t) &= \frac{d}{dt} \int_0^t e(\tau) d\tau = e(t), \\ \dot{x}_2(t) &= \dot{e}(t) = -ae(t) - bu(t - L). \end{aligned}$$

The state space representation yields to

$$\begin{aligned} \dot{x}(t) &= \begin{bmatrix} 0 & 1 \\ 0 & -a \end{bmatrix} x(t) + \begin{bmatrix} 0 \\ -b \end{bmatrix} u(t - L) \\ &= Ax(t) + Bu(t - L). \end{aligned} \quad (4)$$

According to [34], an optimal PI controller for the time delay system (4), which minimizes the quadratic performance index

$$J = \int_0^\infty (x^T(t)Qx(t) + u^T(t)Ru(t))dt, \quad (5)$$

is given by the state feedback control law

$$u(t) = \begin{cases} -Fe^{A_c t} e^{A(L-t)} x(t), & 0 \leq t < L, \\ -Fe^{A_c L} x(t), & t \geq L, \end{cases} \quad (6)$$

where  $F = R^{-1}B^T P$ ,  $P > 0$  is the solution of Riccati's equation  $A^T P + PA - PBB^T R^{-1} B^T P + Q = 0$  [44],  $Q \geq 0$  and  $R > 0$  are the given penalization matrices, with proper dimensions of the performance index (5), and  $A_c = A - BF$ .

With this approach, the eigenvalues of matrix  $Q$  can be calculated as a relationship of the damping ratio  $\zeta$  and natural frequency  $\omega_n$ , which are chosen according to the desire transient response of the second order system (4), as follows

$$\begin{aligned} q_1 &= \frac{\omega_n^4 R}{b^2}, \\ q_2 &= \frac{[(4\zeta^2 - 2)\omega_n^2 - a^2]R}{b^2}. \end{aligned} \quad (7)$$

A steady time  $T_{ss} = 10.7994$  and a maximum overshoot  $M_p = 0.035981\%$  are proposed as design controller parameters, from which  $\zeta$  and  $\omega_n$  could be computed using the relation presented in [46] as  $\omega_n = \frac{4}{\zeta T_{ss}} = 0.3984$  and  $\zeta = \sqrt{\frac{\ln\left(\frac{M_p}{100}\right)^2}{\pi^2 + \ln\left(\frac{M_p}{100}\right)^2}} = 0.9297$ . Then, matrix  $Q = eig\{q_1, q_2\} > 0$ , where  $q_1$  and  $q_2$  are computed from (7) with  $R = 1$ .

Notice that, the control given by equation (6) compensates, relatively easy, the time delay present in the input for  $t < L$ ; and when  $t \geq L$  the control becomes a simple state feedback with the gain vector  $-Fe^{A_c L}$ , whose first component is the integral gain and the second element is the proportional gain. Based on the definition of state variables, the controller is simply  $u(t) = K_i \int_0^t e(\tau) d\tau + K_p e(t)$ .

The controller given by the equation (6) has the advantage to be easily implemented, the gain tuning is related to the time response plant parameters in closed loop.

Although the use of the optimal PI seems to be the best alternative, it is necessary to justify this choice by comparing it with two other PI tuning methods, for which the Ziegler-Nichols and pole assignment methods [47] are chosen. Table IV shows the computed gains for each finger and tuning method. As a side note, pole assignment tuning was performed using  $T_{ss} = 11s$  and  $M_p = 2\%$  (parameters close to those using for PI optimal tuning), while Ziegler-Nichols tuning was calculated using the corresponding formula [47].

TABLE IV  
PI CONTROLLER GAINS COMPUTED FOR EACH FINGER

Finger	Tuning method	Kp	Ki
Index	Optimal PI	3.3672	1.6729
	Pole assignment	4.2069	6.8461
	Ziegler-Nichols	48.4786	0.6967
Middle	Optimal PI	4.4969	1.9782
	Pole assignment	6.0448	8.3278
	Ziegler-Nichols	46.7218	0.8800
Ring	Optimal PI	5.7577	2.6175
	Pole assignment	7.0325	10.5544
	Ziegler-Nichols	105.6059	0.4933
Little	Optimal PI	5.3826	2.2642
	Pole assignment	8.2324	11.2372
	Ziegler-Nichols	57.9882	0.9567
Thumb	Optimal PI	7.5321	3.2483
	Pole assignment	9.3327	13.4201
	Ziegler-Nichols	96.0507	0.6900

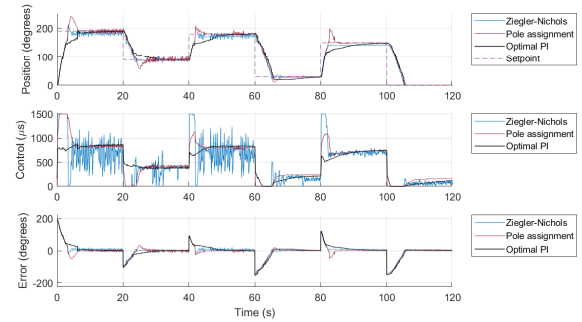
## V. EXPERIMENTAL RESULTS

As mentioned, three tuning methods were compared for the PI controller, the results of that comparison are shown below followed by a test with the grip mode built into the prototype.

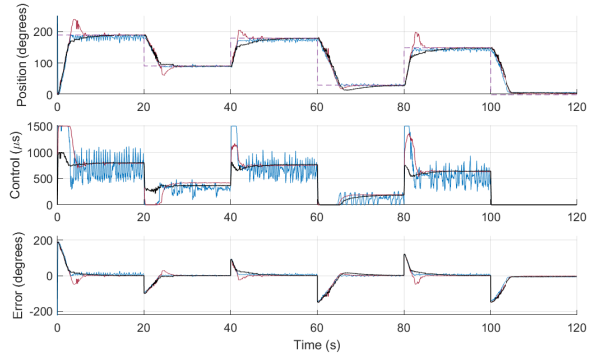
### A. Controller Test

The corresponding computed gains of Table IV, for optimal PI controller, pole assignment and Ziegler-Nichols methods, were loaded into the MCU, using a PID library [48], as well as a random trajectory, composed of various setpoints, for each finger. The objective of the experiment is that the finger position follows the desire setpoints. It is important to note that the resulting values were taken at the same time on all five fingers, showing that they move independently of each other. Figs. 5 and 6 show the fingers' setpoint tracking test. For each finger, position in degrees is depicted in subplot 1, the control signal in subplot 2 is expressed in microseconds ( $\mu s$ ) because it represents the duty cycle of a PWM signal sent to servomotor, and the error signal in subplot 3 is expressed in degrees.

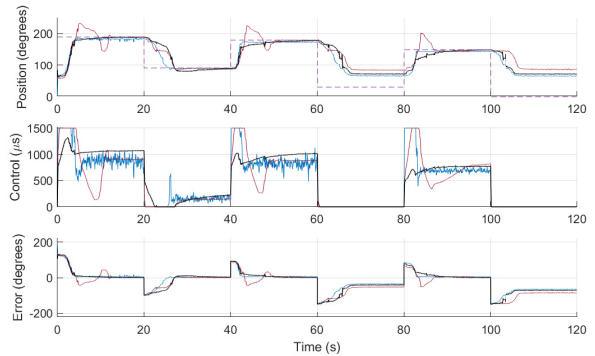
As can be seen, in all three cases, the position of the finger follows the established reference and it is important to notice that the result obtained with the optimal PI tuning method presents a smooth movement and there is no overshoot, which is one of the design objectives of the controller. It can be concluded that the optimal PI strategy fulfils its purpose satisfactorily. Finally, the settle time for each reference is aligned with that established in the controller design, again fulfilling the objective correctly. It is important to mention that even though the method for calculating the linear model is over the operation point, the model is good enough to cover the full range of motion that the fingers have, which is  $0^\circ - 250^\circ$ .



(a) Index finger. Setpoints  $\{190^\circ, 90^\circ, 180^\circ, 30^\circ, 150^\circ, 0^\circ\}$



(b) Middle finger. Setpoints  $\{190^\circ, 90^\circ, 180^\circ, 30^\circ, 150^\circ, 0^\circ\}$



(c) Ring finger. Setpoints  $\{190^\circ, 90^\circ, 180^\circ, 30^\circ, 150^\circ, 0^\circ\}$

Fig. 5. Fingers' setpoint tracking chart (index, middle, ring).

### B. Position and Grip Control

In order to grab an irregular object, an FSR sensor was placed on the palm of the hand and a grip mode was designed. This mode can be enabled or disabled by voice command.

This grip mode consists of an automatic position setpoint adjustment, based on the value read by the sensor. The adjustment stops when the FSR sensor value crosses a predefined threshold. It was set to  $0.1N$ , which is equal to 800 units, which are read through the Analog Digital Converter (ADC) in the MCU.

Fig. 7 shows the automatic adjustment of the setpoint when the optimal PI control is applied; the position of the finger is shown in subplot 1, the force signal in subplot 2, and the control signal in subplot 3 is expressed in microseconds

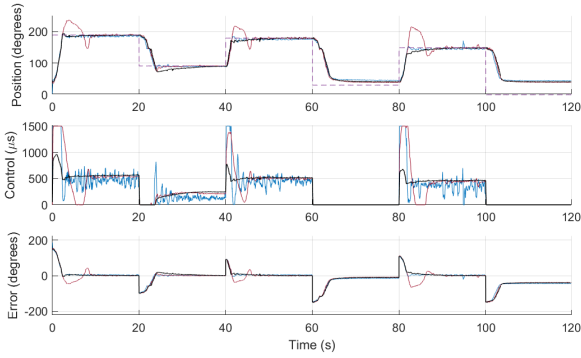
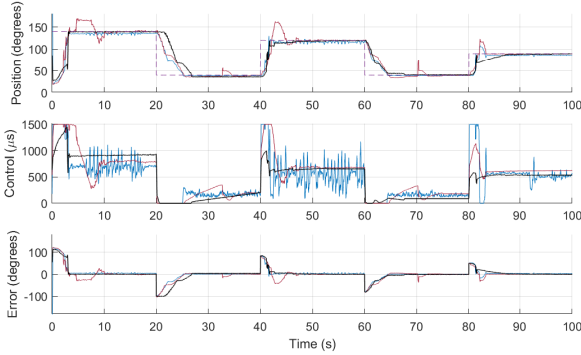
(a) Little finger. Setpoints  $\{190^\circ, 90^\circ, 180^\circ, 30^\circ, 150^\circ, 0^\circ\}$ (b) Thumb. Setpoints  $\{140^\circ, 40^\circ, 120^\circ, 40^\circ, 90^\circ\}$ 

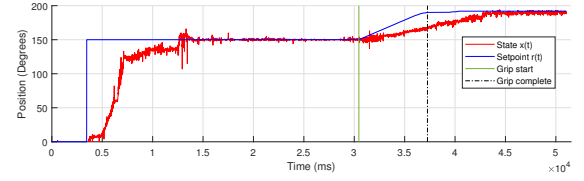
Fig. 6. Fingers' setpoint tracking chart (little, thumb).

( $\mu s$ ) representing the duty cycle of the PWM signal sent to the servomotor. In these plots, the grip start is indicated by the green line, and it is the moment when the grip mode is enabled; which generates an increment of the setpoint. This increase occurs at a rate of  $0.1^\circ$  per task cycle, which is equivalent to  $1^\circ$  every 100ms or  $10^\circ$  per second, this rate was determined heuristically after various tests; the complete grip is showed by the black dashed line, and it is the moment when the force value crosses the threshold and causes the setpoint increment to stop.

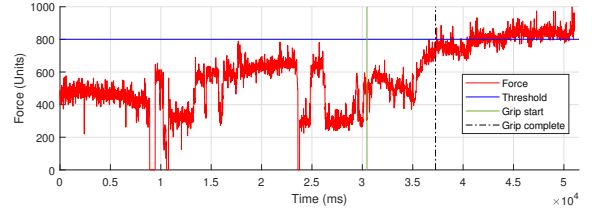
Returning to the results of Fig. 1, it is possible to observe that the hand, using the grasping mode, is capable of gripping irregular objects, both smaller and palm-sized, presenting complications when the objects are larger.

### C. Performance of the Results

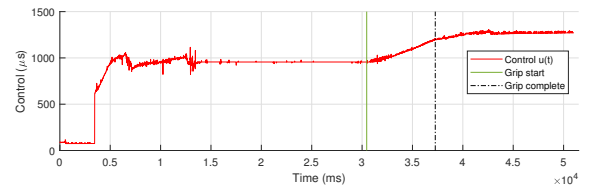
Table V shows the time parameters, obtained when the response of the system was measured (tuned using the three methods described) to a predefined setpoint (same data of Figs. 5 and 6), which allows to evaluate its performance. Maximum overshoot, settle time, and steady-state error were calculated based on the first 20 seconds of the experiment, which are equivalent to a unit step response, while the performance index  $J$ , given by equation (5), was calculated for the total time of the tracking experiment. It is important to mention that the calculation of  $J$  index is carried out with the same  $Q$  and  $R$  penalty matrices employed for computing the gains of



(a) Index finger position



(b) Force



(c) Index finger control

Fig. 7. Position setpoint adjustment by grip control.

the optimal PI controller, being only for comparative purposes.

After analyzing the graphs presented in Figs. 5 and 6 and the data in Table V, it can be seen that the process variable in the three experiments converges to the desire setpoint.

In order to make a comparison on the controls' performance, it is necessary to establish the objectives that the prototype is intended to meet, which are, in order of importance, first, the movement of the finger toward the setpoint must be carried out without (or minimum) overshoot since this would compromise the correct grip of objects. Second, the control signal must have the smallest number and size of oscillations as this causes wear of the actuator. Third, power consumption should be as low as possible in order to maximize battery performance.

For the first criterion, it is observed that the pole assignment control presents an average overshoot of 23.8871%, which is too high for the objectives of the prototype, the optimal PI and Ziegler-Nichols controllers present an average of 1.1776% and 3.0131% respectively, so the optimal PI control is the one that best meets this criterion.

For the second criterion, observing Figs.5 and 6, it is easy to notice that the Ziegler-Nichols tuning presents very marked oscillations resulting in a tremor of the fingers, which is not valid for this criterion. Meanwhile, the remaining controllers present minimal oscillations, both comply with this criterion.

Finally, for the third criterion, a measurement of the current

consumed by the entire system was made, during a period of three minutes, using a current sensor. The result of this experiment is shown in Table VI and it can be seen that the optimal PI controller has lower power consumption than the others. This reinforces the energy usage result. As a side note, using linear extrapolation, it is possible to calculate a system power consumption of 677.5824 mAh. Considering that a standard rechargeable battery has an average capacity of 3500 mAh, it can be inferred that the proposed hand would have an autonomy of approximately five hours.

With all of the above, it is shown that the optimal PI controller is the one that best meets the criteria established for the prototype. Notice that the PI optimal control approach is subject to the quadratic performance index (5), that penalize the state and the control signal with matrix  $Q$  and scalar  $R$ , respectively, which represents a compromise between the use of energy and the state convergence. With this approach the computed  $Q$  and the selected  $R$  allow to obtain a response of desire characteristics ( $T_{ss}$  and  $M_p$ ).

1) *Discussion:* The analysis of the existing literature on robotic hands reveals a notable focus on mechanical design [49]–[51], with relatively limited attention to the control methods. It is apparent that open-loop control predominates in this field [52]–[54]. However, our study introduces a novel approach by presenting the optimal PI control for a robotic hand. In addition, the incorporation of inertial measurement units for finger position determination, alongside the implementation of a non-linkage tendon arrangement, constitutes a substantial breakthrough. This combination effectively addresses a prevailing limitation in the current literature, where fingers with one degree of freedom encounter difficulties in grasping irregular objects [18], [29], [55]. Therefore, the importance of considering advanced control strategies and innovative mechanical configurations in the design and development of future robotic hands is highlighted, leading to enhanced performance, precision, and versatility.

Revisiting the articles shown in Table I, the following advantages and disadvantages are observed concerning the model proposed in this article. The articles [18], [20], [22], [23], [26], [29] exhibit a single degree of freedom and are unable to grasp objects with irregular shapes, a situation addressed in this article by employing the non-linked double-tendon arrangement. On the other hand, the articles [19], [27], [28], [30]–[32] feature a mechanical finger design with more than one degree of freedom, enabling them to grasp objects with irregular shapes. However, they lack a closed-loop control strategy, an aspect that is considered in the present article. Finally, unlike the mentioned articles, the present work conducts an analysis of the energy consumption, demonstrating that the utilized optimal PI control has a lower expenditure compared to the other controls analyzed.

## VI. CONCLUSIONS

This study integrates several components, including an open-source 3D model, an optimal PI control law, a force sensor, inertial measurement units, and parallel multitasking programming techniques, to construct a robotic hand. The conducted experiments demonstrate the capability to maneuver the fingers to desire positions, grasp irregularly shaped objects (even with a single degree of freedom fingers), and reduce energy consumption, facilitated by the use of the optimal PI controller. These findings highlight the feasibility of implementing advanced control techniques and an IoT approach, exemplified by the web application and voice commands, in this type of device. It is observed that the proposed robotic hand exhibits a wide range of movements, within its mechanical constraints, allowing it to grasp diverse shaped objects.

As a prospective avenue for further investigation, the potential redesign of the robotic hand warrants consideration to achieve the 16 grasp positions outlined in the Cutkosky taxonomy. Lastly, there exists an opportunity to implement an online parameter identification strategy with the aim of augmenting the performance of the controller.

## REFERENCES

- [1] A. J. Berger and R. A. Meals, "Management of osteoarthritis of the thumb joints," *The Journal of hand surgery*, vol. 40, no. 4, pp. 843–850, 2015. doi: <https://doi.org/10.1016/j.jhssa.2014.11.026>.
- [2] C. Piazza, G. Grioli, M. G. Catalano, and A. Bicchi, "A century of robotic hands," *Annual Review of Control, Robotics, and Autonomous Systems*, vol. 2, pp. 1–32, 2019. doi: <https://doi.org/10.1146/annurev-control-060117-105003>.
- [3] Robotis, "Robotis." <http://en.robotis.com/>. consulted in 2023.
- [4] Shadow Robot Company, "Shadow robot company." <https://www.shadowrobot.com/>. consulted in 2023.
- [5] Barrett Technology, "Barrett technology." <https://advanced.barrett.com/>. consulted in 2023.
- [6] Robotiq, "Robotiq." <https://robotiq.com/>. consulted in 2023.
- [7] Yujin Robot, "Yujin robot." YujinRobot. consulted in 2023.
- [8] O. Bionics, "Ada robotic hand." <https://www.thingiverse.com/thing:1294517>. consulted in 2023.
- [9] D. Burton, "Robotic or prosthetic hand." <https://www.thingiverse.com/thing:1830958>. consulted in 2023.
- [10] R. Gross, "Humanoid robotic hand." <https://www.thingiverse.com/thing:2269115>. consulted in 2023.
- [11] L. Duran, "Prototype for the lad robotic hand- finger." <https://www.thingiverse.com/thing:3742369>. consulted in 2023.
- [12] L. Riaud, "Robotic hand." <https://www.thingiverse.com/thing:2926729>. consulted in 2023.
- [13] Thingiverse, "Prosthetic hand designs." <https://bit.ly/3LOGUZ5>. consulted in 2023.
- [14] Q. Zhou, N. Jiang, and B. Hudgins, "Improved phoneme-based myoelectric speech recognition," *IEEE Transactions on Biomedical Engineering*, vol. 56, no. 8, pp. 2016–2023, 2009. doi: <https://doi.org/10.1109/TBME.2009.2024079>.
- [15] E. Gruppioni, B. Saldutto, A. Cutti, E. Mainardi, and A. Davalli, "A voice-controlled prosthesis: test of a vocabulary and development of the prototype," *Myoelectric Symposium*, 2008.
- [16] R. Ortega-Palacios, J. Bueno-Lamas, J. Vázquez-López, J. Salgado-Ramírez, I. Ortiz-Hernández, A. Vera, and L. Leija, "Low-cost upper limb prosthesis, based on opensource projects with voice-myoelectric hybrid control," in *2018 Global Medical Engineering Physics Exchanges/Pan American Health Care Exchanges (GMEPE/PAHCE)*, pp. 1–5, IEEE, 2018. doi: <https://doi.org/10.1109/GMEPE-PAHCE.2018.8400727>.



TABLE V  
PERFORMANCE ANALYSIS

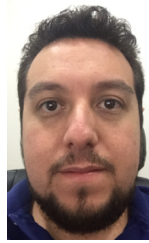
Finger	Tuning method	Performance Index $J$	Maximum overshoot (%)	Settling time (s)	Steady-state error (degrees)
Index	Optimal PI	$76.03 \times 10^6$	2.1381	12.2395	1.9650
	Pole assignment	$85.82 \times 10^6$	26.2828	19.9975	7.7821
	Ziegler-Nichols	$86.72 \times 10^6$	11.7434	19.5460	7.4042
Middle	Optimal PI	$62.55 \times 10^6$	0.1973	9.7007	1.6754
	Pole assignment	$79.50 \times 10^6$	25.9211	14.3554	0.9276
	Ziegler-Nichols	$77.68 \times 10^6$	1.6447	19.8626	7.4000
Ring	Optimal PI	$337.40 \times 10^6$	0.0000	9.7460	1.5417
	Pole assignment	$653.48 \times 10^6$	21.9407	12.2412	0.9974
	Ziegler-Nichols	$229.35 \times 10^6$	0.0000	18.7356	6.5038
Little	Optimal PI	$85.14 \times 10^6$	2.3026	8.9015	1.3753
	Pole assignment	$182.27 \times 10^6$	24.3092	14.8834	1.2120
	Ziegler-Nichols	$99.66 \times 10^6$	1.6776	19.7244	3.5333
Thumb	Optimal PI	$48.13 \times 10^6$	1.2500	3.3393	1.3964
	Pole assignment	$68.44 \times 10^6$	20.9821	10.0434	1.3908
	Ziegler-Nichols	$173.59 \times 10^6$	0.0000	16.9318	4.6329

TABLE VI  
ENTIRE SYSTEM ENERGY CONSUMPTION

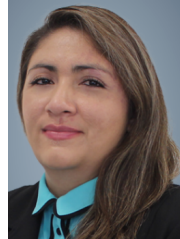
Tuning method	Energy consumption (Wh)
Optimal PI	0.3083
Pole assignment	0.3274
Ziegler-Nichols	0.3376

- [17] Q. K. Pham, T. V. Vo, and P. T. Tran, "On the implementation of a low-cost mind-voice-and-gesture-controlled humanoid robotic arm using leap motion and neurosky sensor," *Journal of Electrical Engineering & Technology*, pp. 1–19, 2022. doi: <https://doi.org/10.1007/s42835-021-00903-5>.
- [18] G. Jang, C. Lee, H. Lee, and Y. Choi, "Robotic index finger prosthesis using stackable double 4-bar mechanisms," *Mechatronics*, vol. 23, no. 3, pp. 318–325, 2013. doi: <https://doi.org/10.1016/j.mechatronics.2013.01.006>.
- [19] X. Li, Q. Huang, X. Chen, Z. Yu, J. Zhu, and J. Han, "A novel underactuated bionic hand and its grasping stability analysis," *Advances in Mechanical Engineering*, vol. 9, no. 2, 2017. doi: <https://doi.org/10.1177/1687814016688859>.
- [20] H. Deng, H. Luo, R. Wang, and Y. Zhang, "Grasping Force Planning and Control for Tendon-driven Anthropomorphic Prosthetic Hands," *Journal of Bionic Engineering*, vol. 15, no. 5, pp. 795–804, 2018. doi: <https://doi.org/10.1007/s42235-018-0067-z>.
- [21] Y.-w. Liu, F. Feng, and Y.-f. Gao, "HIT prosthetic hand based on tendon-driven mechanism," *Journal of Central South University*, vol. 21, no. 5, pp. 1778–1791, 2014. doi: <https://doi.org/10.1007/s11771-014-2124-z>.
- [22] H. Luo, X. Duan, and H. Deng, "Sliding mode impedance control of a underactuated prosthetic hand," in *2014 IEEE International Conference on Information and Automation (ICIA)*, pp. 726–729, IEEE, 2014. doi: <https://doi.org/10.1109/ICInfA.2014.6932747>.
- [23] R. Wang, X. Duan, and H. Deng, "Grasping position estimation for prosthetic hand," in *2015 International Conference on Test, Measurement and Computational Methods*, Atlantis Press, 2015. doi: <https://doi.org/10.2991/tmcm-15.2015.16>.
- [24] G. Langevin, "Inmoov project." <http://inmoov.fr/>. consulted in 2023.
- [25] S. R. Kashef, S. Amini, and A. Akbarzadeh, "Robotic hand: A review on linkage-driven finger mechanisms of prosthetic hands and evaluation of the performance criteria," *Mechanism and Machine Theory*, vol. 145, p. 103677, 2020. doi: <https://doi.org/10.1016/j.mechmachtheory.2019.103677>.
- [26] J. A. Lealndash, C. R. Torres-San Miguel, M. F. Carbajalndash, L. Martinez-Saez, *et al.*, "Structural numerical analysis of a three fingers prosthetic hand prototype," *International Journal of Physical Sciences*, vol. 8, no. 13, pp. 526–536, 2013. doi: <https://doi.org/10.5897/IJPS2013.3824>.
- [27] A. A. M. Faudzi, J. Ooga, T. Goto, M. Takeichi, and K. Suzumori, "Index finger of a human-like robotic hand using thin soft muscles," *IEEE Robotics and Automation Letters*, vol. 3, no. 1, pp. 92–99, 2017. doi: <https://doi.org/10.1109/LRA.2017.2732059>.
- [28] T. Ko, H. Kaminaga, and Y. Nakamura, "Underactuated four-fingered hand with five electro hydrostatic actuators in cluster," in *2017 IEEE International Conference on Robotics and Automation (ICRA)*, pp. 620–625, IEEE, 2017. doi: [doi.org/10.1109/icra.2017.7989077](https://doi.org/10.1109/icra.2017.7989077).
- [29] N. Omarkulov, K. Telegenov, M. Zeinullin, A. Begalinova, and A. Shintemirov, "Design and analysis of an underactuated anthropomorphic finger for upper limb prosthetics," in *2015 37th Annual International Conference of the IEEE Engineering in Medicine and Biology Society (EMBC)*, pp. 2474–2477, IEEE, 2015. doi: [doi.org/10.1109/embc.2015.7318895](https://doi.org/10.1109/embc.2015.7318895).
- [30] D. Yoon and Y. Choi, "Underactuated finger mechanism using contractible slider-crank and stackable four-bar linkages," *IEEE/ASME Transactions on Mechatronics*, vol. 22, no. 5, pp. 2046–2057, 2017. doi: [doi.org/10.1109/tmech.2017.2723718](https://doi.org/10.1109/tmech.2017.2723718).
- [31] M. Cheng, L. Jiang, F. Ni, S. Fan, Y. Liu, and H. Liu, "Design of a highly integrated underactuated finger towards prosthetic hand," in *2017 IEEE International Conference on Advanced Intelligent Mechatronics (AIM)*, pp. 1035–1040, IEEE, 2017. doi: [doi.org/10.1109/aim.2017.8014155](https://doi.org/10.1109/aim.2017.8014155).
- [32] Z. Xu and E. Todorov, "Design of a highly biomimetic anthropomorphic robotic hand towards artificial limb regeneration," in *2016 IEEE International Conference on Robotics and Automation (ICRA)*, pp. 3485–3492, IEEE, 2016. doi: [doi.org/10.1109/icra.2016.7487528](https://doi.org/10.1109/icra.2016.7487528).
- [33] M. S. Bahari, A. Jaffar, C. Y. Low, R. Jaafar, K. Roese, and H. Yussof, "Design and development of a multifingered prosthetic hand," *International Journal of Social Robotics*, vol. 4, no. 1, pp. 59–66, 2012. doi: <https://doi.org/10.1007/s12369-011-0133-8>.
- [34] J.-B. He, Q.-G. Wang, and T.-H. Lee, "PI/PID controller tuning via LQR

- approach,” *Chemical Engineering Science*, vol. 55, no. 13, pp. 2429–2439, 2000. doi: [https://doi.org/10.1016/S0009-2509\(99\)00512-6](https://doi.org/10.1016/S0009-2509(99)00512-6).
- [35] S. I. Yaniger, “Force sensing resistors: A review of the technology,” in *Electro International*, 1991, pp. 666–668, IEEE, 1991. doi: [doi.org/10.1109/electr.1991.718294](https://doi.org/10.1109/electr.1991.718294).
- [36] M. Ceccarelli, N. E. N. Rodriguez, and G. Carbone, “Design and tests of a three finger hand with 1-dof articulated fingers,” *Robotica*, vol. 24, no. 2, pp. 183–196, 2006. doi: <https://doi.org/10.1017/S0263574705002018>.
- [37] ETC2. <https://www.alldatasheet.com/datasheet-pdf/pdf/1132435/ETC2/MG995.html>. consulted in 2023.
- [38] InvenSense, “MPU-6050 Product specification.” <https://invensense.tdk.com/wp-content/uploads/2015/02/MPU-6000-Datasheet1.pdf>. consulted in 2023.
- [39] M. R. Cutkosky *et al.*, “On grasp choice, grasp models, and the design of hands for manufacturing tasks,” *IEEE Transactions on robotics and automation*, vol. 5, no. 3, pp. 269–279, 1989. doi: <http://dx.doi.org/10.1109/70.34763>.
- [40] G. C. Hillar, *MQTT Essentials-A lightweight IoT protocol*. Birmingham, UK: Packt Publishing Ltd, 2017.
- [41] J. Mankar, C. Darode, K. Trivedi, M. Kanoje, and P. Shahare, “Review of I2C protocol,” *International Journal of Research in Advent Technology*, vol. 2, no. 1, 2014.
- [42] Google, “Speech-to-text.” <https://cloud.google.com/speech-to-text>. consulted in 2023.
- [43] D. E. Kirk, *Optimal control theory: an introduction*. Courier Corporation, 2004.
- [44] M. Athans and P. L. Falb, *Optimal control: an introduction to the theory and its applications*. North Chelmsford, Massachusetts: Courier Corporation, 2013.
- [45] L. Rodríguez-Guerrero, O. J. Santos-Sánchez, R. E. Velasco-Rebollo, and C. A. García-Samperio, “Network-based control system to compensate the input delay and minimize energy expenditure of a cooling plant,” in *2018 15th International Conference on Electrical Engineering, Computing Science and Automatic Control (CCE)*, pp. 1–6, IEEE, 2018. doi: [doi.org/10.1109/ICEEE.2018.8533903](https://doi.org/10.1109/ICEEE.2018.8533903).
- [46] W. Bolton, *Instrumentation and control systems*. 8–11 Southampton Street, London: Newnes, 2021. doi: [doi.org/10.1016/b978-0-12-823471-6.00013-7](https://doi.org/10.1016/b978-0-12-823471-6.00013-7).
- [47] K. J. Åström, T. Häggglund, and K. J. Astrom, *Advanced PID control*, vol. 461. Research Triangle Park, NC 27709: ISA-The Instrumentation, Systems, and Automation Society, 2006.
- [48] B. Beauregard, “Arduino pid library - version 1.2.1.” <https://github.com/br3ttb/Arduino-PID-Library>. consulted in 2023.
- [49] T. Asfour and R. Dillmann, “Design of the tuat/karlsruhe humanoid hand,” in *Proceedings of the Second International Symposium Humanoid Robots, Japan*, 2000. doi: <https://doi.org/10.1109/IROS.2000.895225>.
- [50] H. Khakpour and L. Birglen, “Numerical analysis of the grasp configuration of a planar 3-dof linkage-driven underactuated finger,” *Journal of Computational and Nonlinear Dynamics*, vol. 8, no. 2, 2013. doi: <https://doi.org/10.1115/1.4007359>.
- [51] T. Laliberté and C. M. Gosselin, “Underactuation in space robotic hands,” in *Proceeding of the Sixth International Symposium on Artificial Intelligence, Robotics and Automation in Space ISAIRAS: A New Space Odyssey*, 2001.
- [52] D. Mu and Z. Huang, “A new type of parallel finger mechanism,” in *2007 IEEE International Conference on Robotics and Biomimetics (ROBIO)*, pp. 584–588, IEEE, 2007. doi: [doi.org/10.1109/robio.2007.4522227](https://doi.org/10.1109/robio.2007.4522227).
- [53] K. Tae-Uk and O. Yonghwan, “Design of spatial adaptive fingered gripper using spherical five-bar mechanism,” in *Proceedings of the 2014 International Conference on Advanced Mechatronic Systems*, pp. 145–150, IEEE, 2014. doi: [doi.org/10.1109/icamechs.2014.6911640](https://doi.org/10.1109/icamechs.2014.6911640).
- [54] J. Jin, W. Zhang, Z. Sun, and Q. Chen, “Lisa hand: Indirect self-adaptive robotic hand for robust grasping and simplicity,” in *2012 IEEE International Conference on Robotics and Biomimetics (ROBIO)*, pp. 2393–2398, IEEE, 2012. doi: [doi.org/10.1109/robio.2012.6491328](https://doi.org/10.1109/robio.2012.6491328).
- [55] N. E. N. Rodriguez, G. Carbone, and M. Ceccarelli, “Optimal design of driving mechanism in a 1-dof anthropomorphic finger,” *Mechanism and machine theory*, vol. 41, no. 8, pp. 897–911, 2006. doi: [doi.org/10.1016/j.mechmachtheory.2006.03.016](https://doi.org/10.1016/j.mechmachtheory.2006.03.016).



**Erick J. Sánchez-Garnica** is a Ph.D. student in Automation and Control Sciences at the Autonomous University of the State of Hidalgo. He earned a Master’s degree in Science from the Autonomous University of the State of Hidalgo in 2021. His research interests encompass control theory, algorithm implementation on microcontrollers, and software development.



**Liliam Rodríguez-Guerrero** obtained her Ph.D. in Automation and Control Sciences from the Department of Automatic Control at the Center for Research and Advanced Studies of the National Polytechnic Institute in Mexico City in 2016. Since 2017, she has been a research professor at the Autonomous University of the State of Hidalgo and is a member of the National Researchers System at Level I. Her scientific interests encompass systems control with delays, optimal control, and advanced control implementation in industrial controllers.



**Rocío Ortega-Palacios** earned her Ph.D. at the Center for Research and Advanced Studies (CINVESTAV-IPN) in the Department of Electrical Engineering, specializing in Bioelectronics. She is currently a member of the National Researchers System at Level C and has received recognition as a desirable profile from SEP-PRODEP.



**Omar-Jacobo Santos-Sánchez** obtained his Ph.D. in Automation and Control Sciences from the Department of Automatic Control at the Center for Research and Advanced Studies of the National Polytechnic Institute in Mexico City in 2006. Since 2001, he has been a research professor at the Autonomous University of the State of Hidalgo and is a member of the National Researchers System at Level I. His scientific interests encompass systems with delays, optimal control, and nonlinear control.